

GHZ-type and *W*-type entangled coherent states: generation and Bell-type inequality tests without photon counting

Hyunseok Jeong¹ and Nguyen Ba An^{2,3}

¹*Centre for Quantum Computer Technology, Department of Physics,
University of Queensland, Brisbane, Qld 4072, Australia*

²*Institute of Physics and Electronics, 10 Dao Tan, Thu Le, Ba Dinh, Hanoi, Vietnam*

³*School of Computational Sciences, Korea Institute for Advanced Study,
207-43 Cheongryangni 2-dong, Dongdaemun-gu, Seoul 130-722, Korea.*

(Dated: August 8, 2018)

We study *GHZ*-type and *W*-type three-mode entangled coherent states. Both the types of entangled coherent states violate Mermin's version of the Bell inequality with threshold photon detection (i.e., without photon counting). Such an experiment can be performed using linear optics elements and threshold detectors with significant Bell violations for *GHZ*-type entangled coherent states. However, to demonstrate Bell-type inequality violations for *W*-type entangled coherent states, additional nonlinear interactions are needed. We also propose an optical scheme to generate *W*-type entangled coherent states in free-traveling optical fields. The required resources for the generation are a single-photon source, a coherent state source, beam splitters, phase shifters, photodetectors, and Kerr nonlinearities. Our scheme does not necessarily require strong Kerr nonlinear interactions, i.e., weak nonlinearities can be used for the generation of the *W*-type entangled coherent states. Furthermore, it is also robust against inefficiencies of the single-photon source and the photon detectors.

PACS numbers: 03.67.Mn, 42.50.Dv, 03.65.Ud, 42.50.-p

I. INTRODUCTION

Quantum entanglement is a resource for quantum information processing and quantum computing. A large class of entangled states violate Bell-type inequalities [1, 2, 3], which means that the existence of such states cannot be explained by any local theory. It has been known that there exist at least two different types of multipartite entanglement, namely, the *GHZ*-type [4] entanglement and the *W*-type entanglement [5]. These two different types of entanglement are not equivalent and cannot be converted to each other by local unitary operations combined with classical communication [5].

Recently, entangled coherent states (ECSs) [6] in free-traveling optical fields have been found useful to perform tasks such as quantum teleportation [7, 8], quantum computation [9, 10, 11], entanglement purification [12], quantum error corrections [13], etc. Most of these schemes use single-mode coherent-state superpositions (CSSs) as qubits and two-mode ECSs as quantum channels. Recently, Nguyen studied an optimal quantum information processing via multi-mode *W*-type ECSs [8]. In particular, it was shown that there exists a quantum information protocol which can be done only with *W*-type ECSs while *GHZ*-type ECSs fail to accomplish such a task [8]. As an example, the remote symmetric entangling, that allows two distant parties to share a symmetric entangled state, strictly requires *W*-type three-mode ECSs. Even though there have been a number of studies on ECSs revealing their quantum nonlocality [14, 15, 16, 17] and usefulness for quantum information processing [7, 8, 9, 10, 11, 12, 13], most of them have focused on two-mode ECSs while the characteristics of

multi-mode ECSs, particularly the *W*-type ECSs, have been relatively less known.

A *GHZ*-type ECS can be generated using beam splitters with a single-mode CSS. Recently, there have been remarkable theoretical suggestions which are within reach of current technology [18, 19, 20, 21, 22, 23, 24, 25] and an experimental attempt [26] for the generation of single-mode CSSs in free-traveling optical fields. However, the generation of *W*-type ECSs in free-traveling optical fields is not straightforward from single-mode CSSs. Very recently, Yuan *et al.*, suggested a scheme to generate *GHZ*-type and *W*-type ECSs in cavity fields [27]. However, it should be noted that for most of tasks for quantum information processing [7, 8, 9, 10, 11, 12, 13, 14, 15, 16, 17], one needs to generate such ECSs *in free-traveling optical fields*.

In this paper, we suggest a scheme to generate *W*-type ECSs in free-traveling optical fields and study violations of the Mermin's version [28] of the Bell inequality [1] for both the *GHZ*-type and *W*-type ECSs. Our study is closely associated with currently feasible experimental elements in quantum optics. The Bell's inequality test can be performed using linear optics elements and threshold detectors with large violations for *GHZ*-type ECSs but it requires additional nonlinear elements for *W*-type ECSs. As for our generation scheme of *W*-type ECSs, it requires a single-photon source, a coherent state source, beam splitters, phase shifters and threshold photodetectors as well as weak nonlinearities. Our generation scheme is robust against inefficiencies of the single-photon source and the photodetectors.

We organize our paper as follows. In section II we first outline possible schemes to generate multi-mode *GHZ*-type ECSs and then test the Bell-Mermin inequality

for the three-mode case using photon parity (subsection II A) and photon threshold (subsection II B) measurements. Section III also has two subsections. Subsection III A presents a mechanism of generation of three-mode W-type ECS whose violation of the Bell-Mermin inequality is examined in subsection III B by means of photon threshold measurements. Finally, we conclude in section IV.

II. GHZ-TYPE ENTANGLED COHERENT STATES

An N -mode *GHZ*-type ECS is defined as

$$|GHZ, \alpha\rangle = c_1|\alpha, \alpha, \dots, \alpha\rangle_{1\dots N} + c_2|-\alpha, -\alpha, \dots, -\alpha\rangle_{1\dots N} \quad (1)$$

where $|\alpha, \alpha, \dots, \alpha\rangle_{1\dots N} = |\alpha\rangle_1|\alpha\rangle_2\dots|\alpha\rangle_N$ with $|\alpha\rangle_i$ a coherent state of amplitude α while complex coefficients c_1 and c_2 should satisfy the normalization condition. Such an entangled state can be generated with a single-mode CSS

$$|CSS\rangle = c_1|\alpha\rangle + c_2|-\alpha\rangle \quad (2)$$

and beam splitters. Recently, several feasible suggestions have been made for the generation of CSSs in free-traveling optical fields [18, 19, 20, 21, 22, 23, 24, 25]. For example, it was found that simply squeezing a single photon results in a very good approximation of a single-mode CSS with amplitude $\alpha \leq 1.2$ [21]. It was also pointed out that a weak Kerr nonlinearity can be useful to generate CSSs even under realistic decoherence [24]. The beam splitter operator $\hat{B}(r, \phi)$ acting on two arbitrary modes a and b is represented as

$$\hat{B}(r, \phi) = \exp\left\{\frac{\theta}{2}(e^{i\phi}\hat{a}^\dagger\hat{b} - e^{-i\phi}\hat{b}^\dagger\hat{a})\right\}. \quad (3)$$

where the reflectivity r and transmittivity t are determined by θ as

$$r = \sin\frac{\theta}{2}, \quad t = \cos\frac{\theta}{2}, \quad (4)$$

and ϕ specifies the phase difference between the reflected and transmitted fields. We assume $\phi = \pi$ throughout this paper. In particular, if a three-mode *GHZ*-type ECS of the form (1), where $c_1 = -c_2$, needs to be generated, one can pass the CSS, $|\sqrt{3}\alpha\rangle - |-\sqrt{3}\alpha\rangle$ (unnormalized), through two beam splitters BS1 with $r_1 = 1/\sqrt{3}$ and BS2 with $r_2 = 1/\sqrt{2}$ successively as shown in Fig. 1. In general, to generate a *GHZ*-type ECS with an arbitrary mode number N , one should pass a CSS of the form $|\sqrt{N}\alpha\rangle \pm |-\sqrt{N}\alpha\rangle$ through a sequence of $N - 1$ beam splitters with $r_1 = 1/\sqrt{N}$, $r_2 = 1/\sqrt{N-1}$, ... and $r_{N-1} = 1/\sqrt{2}$ or, one can exploit a “tree-scheme” that uses only 50:50 beam splitters combined, if necessary, with state-parity measurements (see, e.g. Ref. [29]).

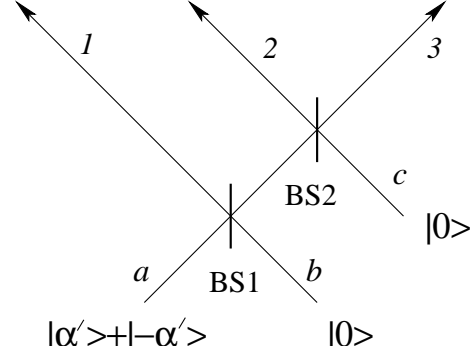


FIG. 1: An example of the generation of a *GHZ*-type three-mode ECS in free-traveling fields from a CSS using two beam splitters, BS1 with $r_1 = 1/\sqrt{3}$ and BS2 with $r_2 = 1/\sqrt{2}$, where r_1 and r_2 are reflectivities of the beam splitters. Note that $\alpha' = \sqrt{3}\alpha$.

A. Bell-inequality violations of *GHZ*-type ECSs using photon parity measurements

We now study the Bell-Mermin inequality for a three-mode *GHZ*-type ECS. Bell inequality violations for two-mode ECSs have been studied with photon parity and photon threshold measurements [16, 17]. We first study the Bell-Mermin inequality based upon the parity measurement and the displacement operation [30]. For that purpose we define an observable $\Pi(\beta)$ as

$$\Pi(\beta) = D(\beta) \sum_{n=0}^{\infty} (|2n\rangle\langle 2n| - |2n+1\rangle\langle 2n+1|) D^\dagger(\beta) \quad (5)$$

where $D(\beta)$ is the displacement operator, $D(\beta) = \exp[\beta\hat{a}^\dagger - \beta^*\hat{a}]$, for bosonic operators \hat{a} and \hat{a}^\dagger . Note that the eigenvalue of the observable $\Pi(\beta)$ is 1 when an even number of photons is detected and it is -1 when an odd number of photons is detected. The Bell-Mermin inequality [1, 28] based on the observable $\Pi(\beta)$ is

$$BM_\Pi = |\langle \Pi(\beta_1)\Pi(\beta_2)\Pi(\beta_3) \rangle - \langle \Pi(\beta_1)\Pi(\beta'_2)\Pi(\beta'_3) \rangle - \langle \Pi(\beta'_1)\Pi(\beta_2)\Pi(\beta'_3) \rangle - \langle \Pi(\beta'_1)\Pi(\beta'_2)\Pi(\beta_3) \rangle| \leq 2, \quad (6)$$

where $\Pi(\beta_1)\Pi(\beta_2)\Pi(\beta_3) = \Pi_1(\beta_1) \otimes \Pi_2(\beta_2) \otimes \Pi_3(\beta_3)$ and we shall call BM_Π the Bell-Mermin function. The average value, $\langle \Pi(\beta_1)\Pi(\beta_2)\Pi(\beta_3) \rangle$, can be calculated using the identity

$$\langle \Pi(\beta_1)\Pi(\beta_2)\Pi(\beta_3) \rangle = \frac{\pi^3}{8} W(\beta_1, \beta_2, \beta_3) \quad (7)$$

where $W(\beta_1, \beta_2, \beta_3)$ represents the Wigner function of the state of interest. The Wigner function of the three-mode *GHZ*-type ECS in Eq. (1), for the case of $c_1 = \pm c_2$, can be calculated as follows [31]. First, the characteristic function $\chi_\pm(\eta_1, \eta_2, \eta_3)$ can be obtained as

$$\chi_\pm(\eta_1, \eta_2, \eta_3) = \text{Tr}[\rho_{GHZ} D(\eta_1) D(\eta_2) D(\eta_3)] \quad (8)$$

where $\rho_{GHZ} = |GHZ, \alpha\rangle\langle GHZ, \alpha|$ and $D(\eta_1)D(\eta_2)D(\eta_3) \equiv D_1(\eta_1) \otimes D_2(\eta_2) \otimes D_3(\eta_3)$. The subscript plus (minus) sign of the characteristic

function in Eq. (8) denotes $c_1 = +c_2$ ($c_1 = -c_2$). The characteristic function is then

$$\begin{aligned} \chi_{\pm}(\eta_1, \eta_2, \eta_3) = & \langle GHZ, \alpha | D(\eta_1)D(\eta_2)D(\eta_3) | GHZ, \alpha \rangle \\ = & M_{\pm} e^{-\frac{1}{2}|\eta_1|^2 - \frac{1}{2}|\eta_2|^2 - \frac{1}{2}|\eta_3|^2} \left(\exp[\eta_1\alpha^* - \eta_1^*\alpha + \eta_2\alpha^* - \eta_2^*\alpha + \eta_3\alpha^* - \eta_3^*\alpha] \right. \\ & + \exp[-\eta_1\alpha^* + \eta_1^*\alpha - \eta_2\alpha^* + \eta_2^*\alpha - \eta_3\alpha^* + \eta_3^*\alpha] \\ & \pm \exp[-6|\alpha|^2 - \eta_1\alpha^* - \eta_1^*\alpha - \eta_2\alpha^* - \eta_2^*\alpha - \eta_3\alpha^* - \eta_3^*\alpha] \\ & \left. \pm \exp[-6|\alpha|^2 + \eta_1\alpha^* + \eta_1^*\alpha + \eta_2\alpha^* + \eta_2^*\alpha + \eta_3\alpha^* + \eta_3^*\alpha] \right) \end{aligned} \quad (9)$$

where $M_{\pm} = 1/(2 \pm 2e^{-6|\alpha|^2})$. The three-mode Wigner function is obtained from the characteristic function as

$$W_{\pm}(\beta_1, \beta_2, \beta_3) = \frac{1}{\pi^6} \int d^2\eta_1 d^2\eta_2 d^2\eta_3 \exp[\eta_1^*\beta_1 - \eta_1\beta_1^* + \eta_2^*\beta_2 - \eta_2\beta_2^* + \eta_3^*\beta_3 - \eta_3\beta_3^*] \chi_{\pm}(\eta_1, \eta_2, \eta_3). \quad (10)$$

After the integration, the Wigner function of the *GHZ*-type ECS is

$$\begin{aligned} W_{\pm}(\beta_1, \beta_2, \beta_3) = & N_{\pm} \left\{ \exp[-2|\beta_1 - \alpha|^2 - 2|\beta_2 - \alpha|^2 - 2|\beta_3 - \alpha|^2] \right. \\ & + \exp[-2|\beta_1 + \alpha|^2 - 2|\beta_2 + \alpha|^2 - 2|\beta_3 + \alpha|^2] \\ \pm & e^{-6|\alpha|^2} \left(\exp[-2(\beta_1 - \alpha)(\beta_1 + \alpha)^* - 2(\beta_2 - \alpha)(\beta_2 + \alpha)^* - 2(\beta_3 - \alpha)(\beta_3 + \alpha)^*] \right. \\ & \left. \left. + \exp[-2(\beta_1 - \alpha)^*(\beta_1 + \alpha) - 2(\beta_2 - \alpha)^*(\beta_2 + \alpha) - 2(\beta_3 - \alpha)^*(\beta_3 + \alpha)] \right) \right\} \end{aligned} \quad (11)$$

with $N_{\pm} = 8/[\pi^3(2 \pm 2e^{-6|\alpha|^2})]$. The Bell-Mermin function BM_{Π} has 12 variables and it is highly nontrivial to find the global maximum values of BM_{Π} for all the 12 variables. Fortunately, some local maximum values which violate the Bell-Mermin inequality can be found numerically using the method of steepest descent [32], which has been plotted in Fig. 2.

Fig. 2 shows that as α increases the value BM_{Π} of the Bell-violation first grows and then asymptotically approaches the value of 3.6 when $\alpha \rightarrow \infty$ for the *GHZ*-type ECSs of $c_1 = c_2$ and $c_1 = -c_2$. For instance, when $\alpha = 10$, the Bell-Mermin function is found to be $BM_{\Pi} \approx 3.58$ at $Re[\beta_1] = Re[\beta_2] = Im[\beta_3] = Re[\beta'_1] = Re[\beta'_2] = Re[\beta'_3] = 0$, $Im[\beta_1] = -Im[\beta'_1] = -0.020$, $Im[\beta_2] = -Re[\beta_3] = -0.0519$ and $Im[\beta'_2] = -Re[\beta'_3] = -0.0259$ for both the cases of $c_1 = c_2$ and $c_1 = -c_2$. It is interesting to note that even when α is extremely small, the *GHZ*-type ECS of $c_1 = -c_2$ (dashed curve in Fig. 2b) still violates the Bell-Mermin inequality whereas the *GHZ*-type ECS of $c_1 = c_2$ does not (solid curve in Fig. 2 b). This is due to the singular behavior of the *GHZ*-type ECS of $c_1 = -c_2$ when α approaches zero. When α approaches zero, the *GHZ*-type ECS becomes a vacuum product state without entanglement, i.e. $|0\rangle|0\rangle|0\rangle$, unless $c_1 = -c_2$. However, if $c_1 = -c_2$, as α ap-

proaches zero, the *GHZ*-type ECS generated using beam splitters as shown in Fig. 1 will approach

$$\frac{1}{\sqrt{3}}(|1\rangle|0\rangle|0\rangle + |0\rangle|1\rangle|0\rangle + |0\rangle|0\rangle|1\rangle) \quad (12)$$

which is a highly nonlocal entangled state. This can be understood as follows. In order to generate the *GHZ*-type ECS of $c_1 = -c_2$ using two beam splitters, BS1 and BS2 as sketched in Fig. 1, a CSS of $c_1 = -c_2$ is needed. The CSS of $c_1 = -c_2$ approaches the single-photon state, $|1\rangle$, for $\alpha \rightarrow 0$ [17]. This single-photon state after passing through BS1 and BS2 in Fig. 1 results in the state given by Eq. (12). Therefore, one can expect that the *GHZ*-type ECS approaches the state (12) showing Bell-type inequality violations only when $c_1 = -c_2$. Such a singular behavior is in agreement with the previous studies for two-mode ECSs [16, 17]. Namely, a two-mode ECS, $|\alpha, \alpha\rangle - |-\alpha, -\alpha\rangle$ (unnormalized), violates the Bell inequality even in the limit $\alpha \rightarrow 0$ because the two-mode ECS becomes a single photon entangled state, $(|0, 1\rangle + |1, 0\rangle)/\sqrt{2}$. Nevertheless, the two-mode ECS, $|\alpha, \alpha\rangle + |-\alpha, -\alpha\rangle$ (unnormalized), ceases to violate the Bell inequality in the limit $\alpha \rightarrow 0$ as in this limit it becomes a vacuum product state $|0\rangle|0\rangle$.

The displacement operation used in this type of Bell-inequality tests can be effectively performed in an optics

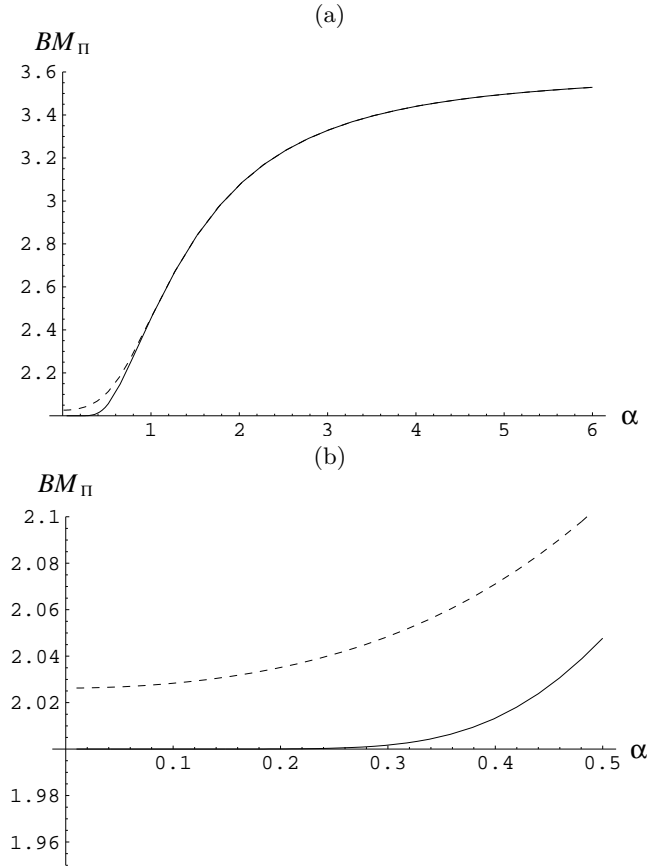


FIG. 2: Violations of Bell-Mermin inequality for the *GHZ*-type ECS of amplitude α using parity measurements. BM_{II} represents the Bell-Mermin function defined in the text which is supposed to be not greater than 2 by a local hidden variable theory. (a) As α increases the violation increases and saturates at ≈ 3.6 for the *GHZ*-type ECSs of $c_1 = c_2$ (solid line) and $c_1 = -c_2$ (dashed line). (b) Even when α is extremely small the *GHZ*-type ECS of $c_1 = -c_2$ (dashed line) still violates the Bell-Mermin inequality while the *GHZ*-type ECS of $c_1 = c_2$ does not.

experiment by means of a beam splitter with the transmission coefficient close to unity and a strong coherent state being injected into the other input port [33]. However, the photon parity measurements should distinguish between odd and even number of photons. This is extremely hard because the detectors which perfectly discriminate between neighbouring photon numbers (i.e. n and $n + 1$ photons) do not exist at the present status of technology. On the other hand, the threshold photon detection, which discriminate between presence and absence of photons, are available with a reasonably high probability using current technology [34]. Therefore, in what follows, we shall focus on the Bell-Mermin inequality test using only threshold photon detection and displacement operations.

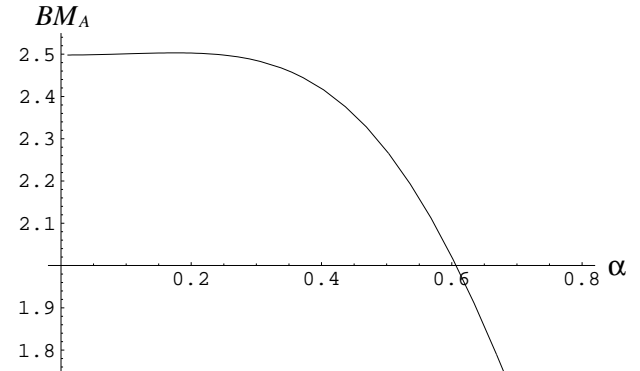


FIG. 3: Violations of Bell-Mermin inequality for a *GHZ*-type ECS of amplitude α using threshold photodetectors. BM_A represents the Bell-Mermin function defined in the text, Eq. (14), which is supposed to be less than or equal to 2 by a local hidden variable theory. As α increases the violation first decreases and then ceases starting from $\alpha \approx 0.6$.

B. Bell-inequality violations of *GHZ*-type ECSs using photon threshold measurements

We define an observable $A(\beta)$ for a Bell-Mermin inequality test with the threshold photon measurements and the displacement operations as

$$A(\beta) = D(\beta)^\dagger (|0\rangle\langle 0| - \sum_{n=1}^{\infty} |n\rangle\langle n|) D(\beta), \quad (13)$$

whose eigenvalue is 1 when no photon are detected and -1 when any $n \geq 1$ photon(s) are detected. The Bell-Mermin inequality based on the observable $A(\beta)$ reads

$$BM_A = |\langle A(\beta_1)A(\beta_2)A(\beta_3) \rangle - \langle A(\beta_1)A(\beta'_2)A(\beta'_3) \rangle - \langle A(\beta'_1)A(\beta_2)A(\beta'_3) \rangle - \langle A(\beta'_1)A(\beta'_2)A(\beta_3) \rangle| \leq 2. \quad (14)$$

In order to calculate BM_A for the ECSs, we first compute the following quantities:

$$J(\beta) \equiv \langle \alpha | A(\beta) | \alpha \rangle = 2 \exp[-|\alpha + \beta|^2] - 1, \quad (15)$$

$$K(\beta) \equiv \langle -\alpha | A(\beta) | -\alpha \rangle = 2 \exp[-|\alpha - \beta|^2] - 1, \quad (16)$$

$$L(\beta) \equiv \langle \alpha | A(\beta) | -\alpha \rangle = \exp[-\frac{1}{2}|\alpha + \beta|^2 - \frac{1}{2}|\alpha - \beta|^2 + \alpha\beta^* - \alpha^*\beta] (2 - e^{-(\alpha+\beta)^*(\alpha-\beta)}). \quad (17)$$

In terms of these quantities we have for the *GHZ*-type three-mode ECS

$$\begin{aligned} \langle A(\beta_1)A(\beta_2)A(\beta_3) \rangle &= |c_1|^2 J(\beta_1)J(\beta_2)J(\beta_3) \\ &+ |c_2|^2 K(\beta_1)K(\beta_2)K(\beta_3) \\ &+ 2\Re[c_1 c_2^* L(\beta_1)L(\beta_2)L(\beta_3)] \end{aligned} \quad (18)$$

from which one can calculate BM_A in Eq. (14). The value of this violation can be found numerically using again the method of steepest descent [32], which has been plotted

for the *GHZ*-type ECSs of $c_1 = -c_2$ in Fig. 3. As can be seen from the figure, the Bell-Mermin inequality is largely violated for a small α . The maximum value is found to be $BM_A \approx 2.5$ when $\alpha \approx 0.18$ at $Re[\beta_1] = Re[\beta_2] = \beta'_2 = \beta'_3 = 0$, $Im[\beta_1] = Im[\beta_2] = -0.371$, $Re[\beta_3] = Im[\beta_3] = -0.295$, and $Re[\beta'_1] = Im[\beta'_1] = 0.173$. Even when α is extremely small, the inequality is still significantly violated because we have considered the *GHZ*-type ECS of $c_1 = -c_2$. As explained in the previous subsection, the *GHZ*-type ECS with this particular relative phase approaches the single photon entangled state (12) for $\alpha \rightarrow 0$. However, the Bell-Mermin inequality ceases to be violated when $\alpha \gtrsim 0.6$ as shown in Fig. 3. Comparing Figs. 2 and 3, we immediately learn that the photon threshold measurements are more efficient to test the Bell-Mermin inequality for *GHZ*-type ECSs with small amplitudes, while the photon parity measurements are more efficient for *GHZ*-type ECSs with large amplitudes.

This result is due to the characteristic of the observable $A(\beta)$ in Eq. (13) composed of the photon threshold measurement and the displacement operations. It should be noted that a Bell-type inequality test depends not only on the state being considered but also on the type of the measurements and the type of the random rotations used for the test. A previous study [17] presents a similar result for nonclassical two-mode fields: two-mode ECSs and two-mode squeezed states significantly violate the Bell-Clauser-Horne inequality [3] using the photon threshold detection and the displacement operations only when the coherent amplitudes (or the degree of squeezing) are small. All these results suggest that the photon threshold measurements and the displacement operations are efficient for a Bell-type inequality test for the continuous variable states only when the average photon number of the states is appropriately small. In this connection, the photon threshold measurements and the displacement operations prove to be very suitable as an efficient tool to test a Bell-type inequality in a quantum optics experiment because *GHZ*-type ECSs with small amplitudes are relatively easy to be generated from CSSs with small amplitudes [21, 24].

III. W-TYPE ENTANGLED COHERENT STATES

A. Generation of *W*-type ECSs

A three-mode *W*-type ECS is [8]

$$|W, \alpha\rangle = a_1|\alpha, -\alpha, -\alpha\rangle_{123} + a_2|-\alpha, \alpha, -\alpha\rangle_{123} + a_3|-\alpha, -\alpha, \alpha\rangle_{123}, \quad (19)$$

where the coefficients should meet the normalization condition. Our *W*-type ECS generation scheme is depicted in Fig. 4. We will first describe how to generate a three-mode *W*-type ECS with $|a_1| = |a_2| = |a_3|$. However, it can be simply generalized to the case with arbitrary

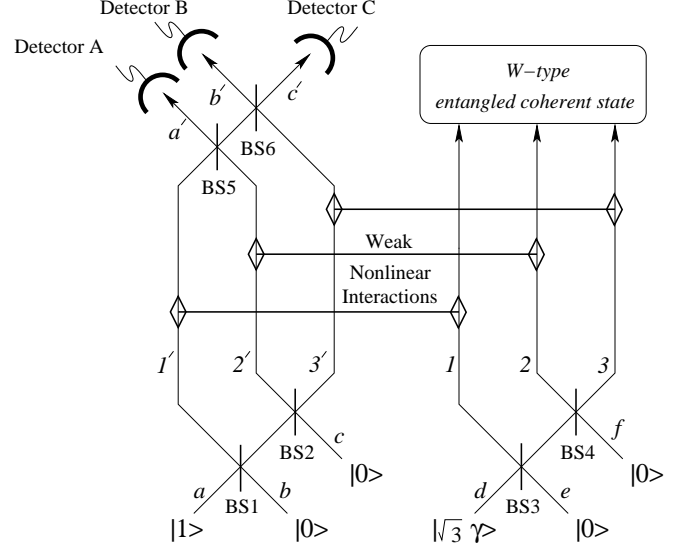


FIG. 4: A schematic of our scheme to generate a *W*-type ECS. A *W*-type ECS is generated when detector B or detector C clicks.

coefficients. In Fig. 4, the reflectivity of the first beam splitter, BS1, is $r_1 = \sqrt{2/5}$ and that of the second beam splitter, BS2, is $r_2 = \sqrt{2/3}$. Through BS1 and BS2, the initial state of the left part in Fig. 4 becomes

$$\hat{B}_{BS2}\hat{B}_{BS1}|1, 0, 0\rangle_{abc} = \frac{1}{\sqrt{5}}(\sqrt{2}|1, 0, 0\rangle + \sqrt{2}|0, 1, 0\rangle + |0, 0, 1\rangle)_{1'2'3'} \quad (20)$$

On the right part of Fig. 4, three coherent states $|\gamma\rangle_1|\gamma\rangle_2|\gamma\rangle_3$ are prepared using a coherent state $|\sqrt{3}\gamma\rangle_d$ and two beam splitters BS3 and BS4 with reflectivities $r_3 = 1/\sqrt{3}$ and $r_4 = 1/\sqrt{2}$, respectively. Then the cross Kerr nonlinear interactions are to be used between mode 1' (2', 3') and mode 1 (2, 3) as shown in Fig. 4. The interaction Hamiltonian of the cross Kerr nonlinear interaction between two arbitrary modes a and b , $H_{CK} = \hbar\chi a^\dagger b^\dagger b$, causes transformations $|0\rangle_a|\gamma\rangle_b \rightarrow |0\rangle_a|\gamma\rangle_b$ and $|1\rangle_a|\gamma\rangle_b \rightarrow |1\rangle_a|\gamma e^{i\theta}\rangle_b$, where $\theta = \chi t$ with χ the coupling constant and t the interaction time. Even though available Kerr nonlinearities are extremely weak, very recently it has been discussed that use of strong coherent fields may circumvent this problem even under realistic assumption of decoherence [24]. Therefore, in our scheme, γ is supposed to be large. The nonlinear interactions transform the total state to

$$\frac{1}{\sqrt{5}}(\sqrt{2}|1, 0, 0\rangle_{1'2'3'}|\gamma e^{i\theta}, \gamma, \gamma\rangle_{123} + \sqrt{2}|0, 1, 0\rangle_{1'2'3'}|\gamma, \gamma e^{i\theta}, \gamma\rangle_{123} + |0, 0, 1\rangle_{1'2'3'}|\gamma, \gamma, \gamma e^{i\theta}\rangle_{123}). \quad (21)$$

Then, two 50:50 beam splitters, BS5 and BS6, are applied to modes 1', 2' and 3' as shown in Fig. 4. It is straightfor-

ward to verify that the total state after passing through

$$\frac{1}{\sqrt{5}}|1,0,0\rangle_{a'b'c'}(|\gamma e^{i\theta}, \gamma\rangle + |\gamma, \gamma e^{i\theta}\rangle)|\gamma\rangle)_{123} + \frac{1}{\sqrt{10}}(|0,1,0\rangle + |0,0,1\rangle)_{a'b'c'}(|\gamma e^{i\theta}, \gamma, \gamma\rangle + |\gamma, \gamma e^{i\theta}, \gamma\rangle + |\gamma, \gamma, \gamma e^{i\theta}\rangle)_{123}. \quad (22)$$

Now, detectors A, B and C (see Fig. 4) are set to detect photons of modes a' , b' and c' , respectively. If detector A clicks the resulting state (unnormalized) is reduced to

$$(|\gamma e^{i\theta}, \gamma\rangle + |\gamma, \gamma e^{i\theta}\rangle)_{12}|\gamma\rangle_3 \quad (23)$$

while either detector B or C clicks it is

$$(|\gamma e^{i\theta}, \gamma, \gamma\rangle + |\gamma, \gamma e^{i\theta}, \gamma\rangle + |\gamma, \gamma, \gamma e^{i\theta}\rangle)_{123}. \quad (24)$$

The final step is to apply the displacement operators, $D(x) \otimes D(x) \otimes D(x)$, with $x = -(\gamma + \gamma e^{i\theta})/2$, on the state in (24). Such operations are to change the state in (24) to the symmetric form in the phase space in Eq. (19). As we have pointed out previously, the displacement operation can be effectively performed using a strong coherent fields (an additional local oscillator in this case) and a biased beam splitter. It can be shown that the final state after the displacement operations is

$$N_W(|\alpha, -\alpha, -\alpha\rangle + |-\alpha, \alpha, -\alpha\rangle + |-\alpha, -\alpha, \alpha\rangle)_{123}, \quad (25)$$

where $\alpha = \gamma(e^{i\theta} - 1)/2$ and $N_W = 1/\sqrt{3 + 6e^{-4|\alpha|^2}}$. However, the final displacement operations are only local unitary transformations which cannot change entanglement nature of a quantum state. Therefore, we stress that the generated state (24) is already a W -type entangled coherent state and the displacement operations mentioned above are just an optional step.

Note that the success probability of getting the W -type three-mode ECS, Eq. (25), is $3/5$, while a two-mode ECS, $(|\alpha, -\alpha\rangle + |-\alpha, \alpha\rangle)_{12}$ (unnormalized), can be obtained with a probability of $2/5$ from the state in Eq. (23) using similar displacement operations. Even though our case concerned $a_1 = a_2 = a_3$, arbitrary values of these coefficients can also be tailored by changing the reflectivities and phases of the beam splitters BS1 and BS2. For example, if one needs to generate a W -type ECS of $a_1 = a_2 = -a_3$, the phase of BS2, ϕ_2 , should be set to be $\phi_2 = \pi$. It is worth emphasizing that our scheme depicted in Fig. 4 does not require highly efficient detectors because the inefficiency of the detectors does not affect the quality of the generated W -type ECSs, yet it might decrease the success probability to be lower than $3/5$. Also of interest is the fact that generally not all the three detectors are necessary in our scheme. For example, only one of the detectors B and C (but not both of them) would suffice to generate a W -type ECS with a success

BS5 and BS6 becomes

probability of $3/10$ when the detector clicks. Furthermore, our scheme is robust to inefficiencies of the single-photon source as well as of the photon detectors. The inefficiencies of the single-photon source and the photon detectors will only reduce the success probability but will not affect the quality of the W -type ECSs to be generated.

B. Bell-inequality violations of W -type ECSs using photon threshold measurements

We now investigate the Bell-Mermin inequality for the W -type ECSs in Eq. (25). According to our numerical study, the Bell-Mermin inequality is not violated for W -type ECSs by the methods used for GHZ -type ECSs in this paper. In this case, the required random rotations for the Bell tests cannot be achieved by the displacement operation [35]. Therefore, in this subsection, we shall alternatively approach the problem by treating the coherent state $|\alpha\rangle$ and the vacuum $|0\rangle$ as a logical qubit basis $\{|0_L\rangle, |1_L\rangle\}$, namely, $|0_L\rangle \equiv |0\rangle$ and $|1_L\rangle \equiv |\alpha\rangle$. Since our approach here becomes a closer analogy of the ideal qubit case for a W -type entangled state [36] when α gets large, it is expected that the Bell-Mermin inequality would strongly be violated in this large- α limit. The first step to make use of the logical qubits is to displace a W -type ECS of the form given by Eq. (25) to a W -type ECS of the following form

$$|\Psi_w\rangle = \mathcal{N}_w(|\alpha, 0, 0\rangle + |0, \alpha, 0\rangle + |0, 0, \alpha\rangle), \quad (26)$$

where $\mathcal{N}_w = 1/\sqrt{3 + 6e^{-|\alpha|^2}}$. This transformation can be done by the local displacement operations $D(\alpha') \otimes D(\alpha') \otimes D(\alpha')$ on a W -type ECSs $|W, \alpha'\rangle$ with $a_1 = a_2 = a_3$, where $\alpha' = \alpha/2$. One can directly transform the state (24) to the state (26) by appropriate displacement operations. Let us introduce a unitary transformation U_X for a coherent-state qubit

$$U_X = D\left(\frac{\alpha}{2}\right)U_K(\pi/\chi)D\left(-\frac{\alpha}{2}\right) \quad (27)$$

where $U_K(t) = e^{iH_K t/\hbar}$, $H_K = \hbar\chi(a^\dagger a)^2$ with t the interaction time in a single-mode Kerr nonlinear medium. In other words, besides the displacement operations, additional single-mode Kerr nonlinear interactions described by the interaction Hamiltonian H_K with the interaction time $t = \pi/\chi$ need to be used for necessary random rotations of a Bell-type inequality test. Even though such

strong nonlinear interactions are very demanding in a real experiment, there was an experimental report for a successful measurement of giant Kerr nonlinearity [37]. Using the identity [38], $U_K(\pi/\chi)|\alpha\rangle = e^{-i\pi/4}(|\alpha\rangle + i|\alpha\rangle)/\sqrt{2}$, one can easily verify

$$\begin{aligned} U_X|0\rangle &= \frac{e^{-i\pi/4}}{\sqrt{2}}(|0\rangle + i|\alpha\rangle), \\ U_X|\alpha\rangle &= \frac{e^{-i\pi/4}}{\sqrt{2}}(i|0\rangle + |\alpha\rangle). \end{aligned} \quad (28)$$

which corresponds to $-\pi/2$ rotation around the x axis up to the irrelevant global phase factor for the qubit basis $\{|0\rangle, |\alpha\rangle\}$. Because of the additional Kerr nonlinearities used, we define an observable $\mathcal{A}(\tau)$, which is slightly different from $A(\beta)$ in Eq. (13):

$$\mathcal{A}(\tau) = U(\tau)^\dagger(|0\rangle\langle 0| - \sum_{n=1}^{\infty} |n\rangle\langle n|)U(\tau), \quad (29)$$

where τ is either 0 or 1 and

$$U(0) = \mathbb{1}, \quad U(1) = U_X. \quad (30)$$

When α is large, the states $|0\rangle$ and $|\alpha\rangle$ are eigenstates of the observable $\mathcal{A}(0)$ with the eigenvalues 1 and -1 , respectively. The Bell-Mermin inequality is then constructed as

$$\begin{aligned} BM_{\mathcal{A}} &= |\langle \mathcal{A}(\tau_1)\mathcal{A}(\tau_2)\mathcal{A}(\tau_3) \rangle - \langle \mathcal{A}(\tau_1)\mathcal{A}(\tau'_2)\mathcal{A}(\tau'_3) \rangle \\ &\quad - \langle \mathcal{A}(\tau'_1)\mathcal{A}(\tau_2)\mathcal{A}(\tau'_3) \rangle - \langle \mathcal{A}(\tau'_1)\mathcal{A}(\tau'_2)\mathcal{A}(\tau_3) \rangle| \leq 2. \end{aligned} \quad (31)$$

Taking $\tau_1 = \tau_2 = \tau_3 = 0$ and $\tau'_1 = \tau'_2 = \tau'_3 = 1$, and using Eqs. (26) to (30), it is straightforward to calculate

$$\langle \mathcal{A}(0)\mathcal{A}(0)\mathcal{A}(0) \rangle = \frac{4 - e^{\alpha^2}}{2 + e^{\alpha^2}} \equiv \mathcal{V}(\alpha) \quad (32)$$

and

$$\begin{aligned} \langle \mathcal{A}(0)\mathcal{A}(1)\mathcal{A}(1) \rangle &= \langle \mathcal{A}(1)\mathcal{A}(0)\mathcal{A}(1) \rangle = \langle \mathcal{A}(1)\mathcal{A}(1)\mathcal{A}(0) \rangle \\ &= -\frac{2 - 2e^{-2\alpha^2} - 7e^{-\alpha^2} - 2e^{\alpha^2}}{3(2 + e^{\alpha^2})} \equiv \mathcal{W}(\alpha) \end{aligned} \quad (33)$$

where α was assumed to be real. Then the Bell-Mermin function is obtained as

$$\begin{aligned} BM_{\mathcal{A}} &= |\mathcal{V}(\alpha) - 3\mathcal{W}(\alpha)| \\ &= \left| \frac{6 - 2e^{-2\alpha^2} - 7e^{-\alpha^2} - 3e^{\alpha^2}}{2 + e^{\alpha^2}} \right| \end{aligned} \quad (34)$$

The Bell-Mermin function $BM_{\mathcal{A}}$ has been plotted in Fig. 5. The Bell-Mermin inequality begins to be violated from $\alpha \approx 1.49$ and the value of $BM_{\mathcal{A}}$ rapidly saturates to 3 as α grows.

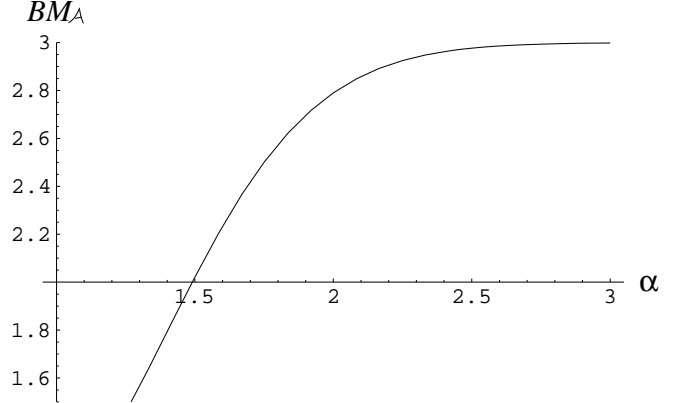


FIG. 5: Violations of the Bell-Mermin inequality for a W -type ECS of amplitude α using threshold photodetectors and nonlinear interactions. The Bell-Mermin function $BM_{\mathcal{A}}$ is larger than the classical bound 2 for $\alpha \gtrsim 1.49$.

IV. CONCLUSION

We have studied Mermin's version of the Bell inequality for GHZ -type and W -type three-mode ECSs. Both the types of ESCs violate the Bell-Mermin inequality with threshold photon detection (i.e., without photon counting). Such an experiment can be performed using linear optics elements and threshold detectors with large violations for GHZ -type ESCs. However, it would be experimentally more difficult to demonstrate Bell-type inequality violations for W -type ECSs since it requires additional strong nonlinear interactions. We have found out that the photon threshold measurements are more efficient to test the Bell-Mermin inequality for the GHZ -type ECSs of small amplitudes, but for the W -type ECSs of large amplitudes: an interesting fact that reflects a clear inequivalence between the two types of ECSs. The generation of a GHZ -type ECS requires a CSS and two beam splitters. Recently, there was an experimental report to generate a CSS in a real laboratory even though the fidelity was limited [26]. Based on the recent theoretical [18, 19, 20, 21, 22, 23, 24, 25] and experimental [26] progress, it is expected that the realization of a CSS with higher fidelity can be achieved in the foreseeable future.

We have also proposed, for the first time, a scheme to generate W -type ECSs for three free-traveling optical fields (generalization to more than three fields is possible). The required resources are a single-photon source, a coherent state source, beam splitters, phase shifters, photodetectors, and Kerr nonlinearities. Our scheme does not necessarily require strong Kerr nonlinear interactions, i.e., weak nonlinearities can be useful for our scheme. Furthermore, it is also robust against inefficiencies of the single-photon source and the photon detectors.

It should be noted that good mode matching would be required at BS5 and BS6 in Fig. 4, while efficient mode matching between optical fields at a beam splitter is being performed in a real laboratory condition using

present technology [39]. The dark count rate of photodetectors will affect the fidelity of the generated W -type ECSs. Currently, highly efficient detectors have relatively high dark count rates while less efficient detectors have very low dark count rates [34]. We emphasize that our scheme here does not require highly efficient detectors. Compared with the scheme to generate a CSS with only one weak nonlinear interaction [24], from which the generation of GHZ -type ECSs can be straightforwardly performed, the most demanding element in our scheme would be to control the three weak nonlinear interactions

in Fig 4. However, such techniques using weak nonlinearities are being intensively studied [24, 25, 40, 41].

Acknowledgments

H.J. is supported by the Australian Research Council while N.B.A. by the Vietnam Institute of Physics and Electronics and Korea Institute for Advanced Study.

[1] S. Bell, Physics **1**, 195 (1964).

[2] J. F. Clauser, M. A. Horne, A. Shimony and R. A. Holt, Phys. Rev. Lett. **23**, 880 (1969).

[3] J. F. Clauser and M. A. Horne, Phys. Rev. D **10**, 526 (1974).

[4] D. M. Greenberger, M. A. Horne, and A. Zeilinger, *Bell's theorem, Quantum theory, and Conceptions of the the Universe*, ed. M. Kafatos, Kluwer, Dordrecht, 69 (1989);

[5] W. Dür, G. Vidal, and J. I. Cirac, Phys. Rev. A **62**, 062314 (2000).

[6] B. C. Sanders, Phys. Rev. A **45**, 6811 (1992).

[7] S.J. van Enk and O. Hirota, Phys. Rev. A **64**, 022313 (2001); H. Jeong, M.S. Kim, and J. Lee, Phys. Rev. A **64**, 052308 (2001); X. Wang, Phys. Rev. A **64**, 022302 (2001); Nguyen Ba An, Phys. Rev. A **68**, 022321 (2003).

[8] Nguyen Ba An, Phys. Rev. A **69**, 022315 (2004).

[9] H. Jeong and M.S. Kim, Phys. Rev. A **65**, 042305 (2002).

[10] T.C. Ralph, W.J. Munro, and G.J. Milburn, Proceedings of SPIE **4917**, 1 (2002).

[11] T.C. Ralph, A. Gilchrist, G.J. Milburn, W.J. Munro, and S. Glancy, Phys. Rev. A **68**, 042319 (2003).

[12] H. Jeong and M.S. Kim, Quantum Information and Computation **2**, 208 (2002); J. Clausen, L. Knöll, and D.-G. Welsch, Phys. Rev. A **66**, 062303 (2002).

[13] P.T. Cochrane, G.J. Milburn, and W.J. Munro, Phys. Rev. A **59**, 2631 (1999); S. Glancy, H.M. Vasconcelos, and T.C. Ralph, Phys. Rev. A **70**, 022317 (2004).

[14] A. Mann, B. C. Sanders and W. J. Munro, Phys. Rev. A **51**, 989 (1995).

[15] J. Wenger, M. Hafezi, F. Grosshans, R. Tualle-Brouri, and P. Grangier, Phys. Rev. A **67**, 012105 (2003).

[16] D. Wilson, H. Jeong and M. S. Kim, J. Mod. Opt., **49**, Special issue for QEP 15, 851 (2002).

[17] H. Jeong, W. Son, M. S. Kim, D. Ahn and C. Brukner, Phys. Rev. A **67**, 012106 (2003).

[18] F. De Martini, Phys. Rev. Lett **81**, 2842 (1998); F. De Martini, M. Fortunato, P. Tombesi, and D. Vitali, Phys. Rev. A **60**, 1636 (1999).

[19] M. Dakna, J. Clausen, L. Knöll and D. -G. Welsch, Phys. Rev. A **59**, 1658 (1999); J. Clausen, M. Dakna, L. Knöll and D.-G. Welsch, Optics Communications **179**, 189 (2000).

[20] M. Paternostro, M.S. Kim, and B.S. Ham, Phys. Rev. A **67**, 023811 (2003); M. Paternostro, M.S. Kim, and B.S. Ham, J. Mod. Opt. **50**, 2565 (2003).

[21] A.P. Lund, H. Jeong, T.C. Ralph, and M.S. Kim, Phys. Rev. A **70**, 020101(R) (2004); H. Jeong, A.P. Lund, T.C. Ralph, Phys. Rev. A **72**, 013801 (2005).

[22] H. Jeong, M. S. Kim, T. C. Ralph, and B. S. Ham, Phys. Rev. A **70**, 061801(R) (2004).

[23] B. Wang and L.-M. Duan, Phys. Rev. A **72**, 022320 (2005).

[24] H. Jeong, Phys. Rev. A **72**, 034305 (2005).

[25] M. S. Kim and M. Paternostro, quant-ph/0510057.

[26] J. Wenger, R. Tualle-Brouri, and P. Grangier, Phys. Rev. Lett **92**, 153601 (2004).

[27] C.-H. Yuan, Y.-C. Ou and Z.-M. Zhang, quant-ph/0509069.

[28] N. D. Mermin, Phys. Rev. Lett. **65**, 1838 (1990).

[29] Nguyen Ba An and J. Kim, quant-ph/0303149.

[30] K. Banaszek and K. Wódkiewicz, Phys. Rev. A **58**, 4345 (1998); Phys. Rev. Lett. **82**, 2009 (1999).

[31] D.F. Walls and G.J. Milburn, *Quantum Optics*, Springer-Verlag (1994).

[32] W. H. Press, B. P. Flannery, S. A. Teukolsky and W. T. Vetterling, *Numerical Recipes* (Cambridge University Press, Cambridge, 1988).

[33] H. M. Wiseman and G. J. Milburn, Phys. Rev. Lett. **70**, 548 (1993); K. Banaszek and K. Wódkiewicz, Phys. Rev. Lett. **76**, 4344 (1996); S. Wallentowitz and W. Vogel, Phys. Rev. A **53**, 4528 (1996).

[34] S. Takeuchi, J. Kim, Y. Yamamoto, and H.H. Hogue, Appl. Phys. Lett. **74**, 1063 (1999).

[35] C. Wu, J.-L. Chen, L. C. Kwek and C. H. Oh, quant-ph/0510013; In this very recent preprint, the authors studied quantum nonlocality of N -qubit W -type entangled states, where a Bell violation for three-mode W -type single-photon entangled states, $(|1, 0, 0\rangle + |0, 1, 0\rangle + |0, 0, 1\rangle)/\sqrt{3}$, was not found using the parity measurements and the displacement operations. The author pointed out that this could be due to “displacement measurements” on the particles, which is in accordance with our understanding.

[36] A. Cabello, Phys. Rev. A **65**, 032108 (2002).

[37] L. V. Hau, S. E. Harris, Z. Dutton, and C. H. Behroozi, Nature **397**, 594 (1999).

[38] B. Yurke and D. Stoler, Phys. Rev. Lett. **57**, 13 (1986).

[39] T. B. Pittman and J. D. Franson, Phys. Rev. Lett. **90**, 240401 (2003).

[40] J. Fiurášek, L. Mišta, and R. Filip, Phys. Rev. A **67**, 022304 (2003); H. Jeong, PhD thesis, Queen's University Belfast, UK (2003); S. D. Barrett, P. Kok, K. Nemoto, R. G. Beausoleil, W. J. Munro, and T. P. Spiller, Phys. Rev. A **71**, 060302(R) (2005).

[41] K. Nemoto and W. J. Munro Phys. Rev. Lett. **93**, 250502 (2004); W. J. Munro, K. Nemoto and T. Spiller, New J. Phys. **7**, 137 (2005).